



Efficiency of rubber-pad cushion in bending process of a thin aluminum sheet

L. Ben Said^{1,3} · M. Wali^{2,3} · N. Khedher¹ · A. Kessentini^{2,3} · A. Algahtani² · F. Dammak³

Received: 3 May 2019 / Accepted: 6 May 2020
© The Malaysian Rubber Board 2020

Abstract

The present paper presents numerical and experimental comparative studies between the conventional bending process (bending using punch and V-die) and bending with a rubber-pad cushion. In fact, a finite-element method is introduced to compare these two procedures used to bend AA1050-H14 Aluminum thin sheet. An elastoplastic constitutive model with quadratic yield criterion of Hill 48 and isotropic hardening behavior has been adopted in FE simulations performed using ABAQUS explicit. To model rubber material, a Mooney–Rivlin theory is used in the finite-element simulation. The purpose of this study is to see the difference between the two methods in terms of effort evolution, springback, stress distribution, thinning. Analyze the effect of the rubber material; in fact, natural rubber, and polyurethane with hardness 50, 70, and 90 shore A are investigated. This numerical study was validated by an experimental investigation that proved the efficiency of the elastic cushion to bend in a better way this thin aluminum sheet.

Keywords Bending · Rubber-pad cushion · Die · Springback · Mooney–rivlin

Introduction

The transformation of a thin sheet into finished products is of considerable importance in many industries such as automotive and aeronautics. The premature tearing of sheet manufactured by means of bending process is one of the major problems currently encountered by the industry working this type of process. Scientists and industrialists are, therefore, always looking for the best conditions for which the ability to deform sheet can go to its maximum to minimize rejects. The economic and technological advantages of the bending process are undeniable: high production rates, geometric and mechanical quality of parts, and low rate of rejects. The difficulty in implementing this process is related to the sensitivity of the forming operation to many

parameters. In fact, the setup of the bending operation is sometimes widely so long and costly. The use of flexible materials was introduced in the conventional sheet forming processes that use plastic deformation like deep drawing, stamping, and bending process. Indeed, used as punches or dies, elastomeric materials make it possible to obtain parts having complex shapes, without the need to change these tools when the shape changes. It has the advantage to avoid wrinkling, fractures usually encountered in conventional metal-forming processes, shorten the production preparation cycle, lessen the springback, and improve the surface quality [1]. This forming process was subsequently developed to be used in the fields of aerospace and automotive with different techniques. That consists of using an elastomeric material between the punch and the sheet or between the sheet and the die. Flexible forming with rubber pad presents many advantages compared with conventional forming. In this kind of process, the same soft tool may be used for several types of different parts, the alignment problems of punch–die are eliminated, and the surface finish of the manufactured parts is improved.

In the context of research, numerical simulations using the finite-element method are used to deal with various difficulties related to problems encountered in sheet metal-forming processes in general and especially in bending

✉ L. Ben Said
bensaid_rmq@yahoo.fr

¹ Mechanical Engineering Department, College of Engineering, Hail University, Hail, Saudi Arabia

² Department of Mechanical Engineering, College of Engineering, King Khalid University, Abha, Saudi Arabia

³ Laboratory of Electro-Mechanical Systems (LASEM), National Engineering School of Sfax, University of Sfax, 3038 Sfax, Tunisia

operation. Giuseppe [1] and Alberti et al. [2], respectively, optimized the rubber forming process by numerical simulations. Their investigations exposed the effectiveness of FEM in rubber forming process design. However, FEM concerning the rubber forming process is not so effective compared to the traditional sheet metal-forming process with a rigid die, because of the complicated deformation of rubber [3, 4]. Dirikolu and Akdemir [3] used the finite-element simulation method to optimize parameters of a flexible forming process such as contact friction, the rubber hardness, rubber material type, etc.... those parameters that require an adjustment before the execution of the forming operation. They considered that polyurethane with a hardness between 55 and 70 shore A is the suitable material for the flexible forming process. The rubber hardness is the most concerned process parameter that must be detailed [4]. In Quadrini et al. [5], authors tested three tools made of silicone rubber, styrene butadiene, and polyamide 66. They concluded that the hardest material (PA66) gives the best stamping results. Liu et al. [6] have investigated the forming of a bipolar plate by rubber-pad forming process using a 2D simulation. The simulations are used for quality control and problem analysis such as tearing, wrinkling, and surface distortion. The same parameter was investigated also in Young-na et al. [7]. Belhassen et al. [8] proved that the use of polyurethane rubber as a soft punch is recommended to minimize the springback of the aluminum sheet when comparing to the natural rubber (NR). Besides, polyurethane rubber with a less hardness value may delay the occurrence of damage. The usefulness of such analysis is limited by the accuracy of the description of the friction phenomena in the sheet/tool contact area [9]. Browne and Battikha [10] investigated the lubricated contact in the Guerin process. They showed through an experimental study that the correct choice of lubricant was necessary for the manufacture of AA1200-H14 aluminum alloy with elastic tools such as neoprene. The wax lubricant (Vestoplast 703) is better suited for the forming operation compared to the oil, as regards the quality of the finished parts.

Sheet metal bending using rubber-pad tools is very widely used in industry in many applications such as aircraft manufacturing and automotive. However, the amount of research work studying this process remains few and may be insufficient [11]. Arnet [12] used a rubber-pad cushion as the lower die, in a roller bending process. In fact, he concluded that the rubber pad has better fatigue characteristics than conventional die materials. Kwon et al. [13] have conducted investigations on the process design of the roller bending of a structural frame of AA6061-T6 with a vulcanized polyurethane rubber pad with hardness 60 shore A. From the experimental study, authors proved that the number of cycles has a minimal influence when it is compared with the effect of the roller path used in this bending process. Several investigations on the roller bending process with its

different categories (conventional roller bending, incremental roller bending, etc.) have been detailed in [14–16]. Lee et al. [17] conducted investigations on the bending process of aluminum tubes using rubber tools. They found that rubber with low hardness values might decrease the minimum radius of curvature of the manufactured tube. Liu et al. [18] studied the manufacture of channels on the metal bipolar plate with a flexible die. Two deformation styles (convex and concave) were analyzed. As a conclusion, they confirmed that the thickness distribution became more uniform when the convex deformation style is performed.

Springback phenomena are one of the major problems encountered in the bending process. Chen et al. [19] studied springback to confirm that this parameter decreases when sheet thickness increases and increases when the die-bending radius increases. They concluded also that the increase of the pressure and the bending time during a bending process with elastomeric tools has not a remarkable effect on the springback compared to its effect in the conventional bending. Liu et al. [20] investigated bending with elastic tools in warm conditions. They indicated that heating-assisted laser-driven soft punch micro-forming would be a good choice to improve the micro-forming abilities of sheet metal laminates. In Jin et al.'s [21] study, a rubber forming method is used to manufacture titanium bipolar plates for proton exchange membrane fuel cells. The optimum-forming conditions are found to be a rubber thickness of 10 mm, rubber hardness equivalent to that of Shore A 20, punch velocity of 30 mm/s, punch pressure of 55 MPa. Lee et al. [17] developed an experimental setup to investigate deformation characteristics of an extruded rectangular aluminum tube in rubber-pad bending. Authors proved that to decrease the minimum formable radius of curvature of tubes while maintaining bending rigidity suitable for a structural use, the roller diameter should be increased and the rubber hardness decreased. The last parameter was a dominant process parameter that affected the cross-sectional deformation of the rectangular tube.

The idea of conducting such a detailed study on application of rubber-pad cushion in bending process stems from the lack of advanced studies on this subject, like those developed in the conventional stamping process. In fact, from the previous state of art, it is denoted that the amount of research work studying this process remains few and may be insufficient. In this study, the rubber-pad bending of AA1050-H14 aluminum sheet metal is investigated through numerical and experimental studies. The effect of the rubber hardness and type on the evolution of effort, stress distribution, formability, thinning, and springback phenomenon was investigated. An elastoplastic constitutive model with quadratic yield criterion of Hill 48 and isotropic hardening behavior has been adopted for the aluminum blank. A Mooney–Rivlin theory is used to model the hyper-elastic behavior of rubber.

Finite-element simulations using ABAQUS explicit are used to predict the different parameters cited previously. Experimental results are used to validate the numerical study, and these results proved the efficiency of the elastic cushion to bend in a better way thin aluminum sheet.

Constitutive model

Elasto-plastic model

This section develops the formulation of the constitutive elastoplastic equations (detailed in [22–34]) to model anisotropic yielding, and non-linear isotropic hardening used to simulate thin sheets manufactured by plastic deformation considered in sheet forming process, such as stamping and bending. The integration scheme used is based on the elastic prediction–plastic correction method. This modeling will be done in the spirit of being able to implement it later in the ABAQUS finite-element code.

To model the materials' mechanical behavior, the relationship between stress and strain should be established. It is assumed that hypo-elastic stress–strain relation can be written as:

$$\dot{\sigma}_{ij} = D_{ijkl} \dot{\epsilon}_{kl}^e, \quad (1)$$

where $\dot{\sigma}$ is the material time derivative of the Cauchy stress tensor, $\dot{\epsilon}^e$ is the elastic part of the strain rate tensor, and \mathbf{D} is the Hooke stress–strain tensor. For isotropic elasticity, tensor \mathbf{D} is given in terms of the shear modulus G and Poisson's ratio ν by:

$$D_{ijkl} = 2G \left(\delta_{ik} \delta_{jl} + \frac{\nu}{1-2\nu} \delta_{ik} \delta_{jl} \right). \quad (2)$$

Moreover, the following assumption of strain rate decomposition is assumed:

$$\dot{\epsilon} = \dot{\epsilon}^e + \dot{\epsilon}^p, \quad (3)$$

where $\dot{\epsilon}$ is the strain rate tensor, $\dot{\epsilon}^p$ is the plastic part of the strain rate tensor, and $\dot{\epsilon}^e$ is the elastic part of the strain rate tensor.

Also, we consider the one of the most common yield criteria that is used in the simulation of forming processes, Hill'48 [35] quadratic yield function, which is given, with isotropic hardening, as follows:

$$f = \varphi(\sigma) - [\sigma_y + R(\kappa)], \quad \varphi(\sigma) = \sqrt{\sigma^T \mathbf{P} \sigma} \quad (4)$$

where σ_y is the initial yield stress, κ models the isotropic hardening, and \mathbf{P} is a fourth-order tensor which defines the yield criterion. This yield function includes the classical

J_2 plasticity yield condition. The Hill'48 yield criterion, in three-dimensional cases, is obtained by taking:

$$[\mathbf{P}] = \begin{bmatrix} H+G & -H & -G & 0 & 0 & 0 \\ & H+F & -F & 0 & 0 & 0 \\ & & F+G & 0 & 0 & 0 \\ & & & 2N & 0 & 0 \\ & \text{Sym} & & & 2M & 0 \\ & & & & & 2L \end{bmatrix}, \quad (5)$$

where F , G , H , N , M , and L are material constants obtained by tests of the material in different orientations.

Moreover, with the hypotheses of associated plasticity, the flow rule is given by:

$$\dot{\epsilon}^p = \dot{\gamma} \frac{\partial f}{\partial \sigma} = \dot{\gamma} n, \quad n = \frac{1}{\varphi} \mathbf{P} \sigma, \quad (6)$$

where $\dot{\gamma}$ denotes the plastic multiplier. In Eq. (4), κ is given by:

$$\dot{\kappa} = -\dot{\gamma} \frac{\partial f}{\partial R} = \dot{\gamma}. \quad (7)$$

Finally, the loading/unloading conditions, formulated in standard Kuhn–Tucker form, are as follows:

$$f \leq 0, \quad \dot{\gamma} \geq 0, \quad \dot{\gamma} f = 0. \quad (8)$$

Integration algorithm

The plastic strain ϵ_{n+1}^p are determined by the integration of the flow rule over a time step. The integration is made using the implicit Euler method. This leads to:

$$\epsilon_{n+1}^p = \epsilon_n^p + \Delta\gamma \mathbf{n}_{n+1}, \quad (9)$$

$$\text{where } \mathbf{n}_{n+1} = \frac{1}{\varphi_{n+1}} \mathbf{P} \sigma_{n+1}. \quad (10)$$

Using Eqs. (3) and (9) into the stress–strain relation, Eq. (1) gives the stress tensor as:

$$\sigma_{n+1} = \sigma^{tr} - \Delta\gamma \mathbf{D} \mathbf{n}_{n+1}, \quad (11)$$

where σ^{tr} is the elastic trial stress:

$$\sigma^{tr} = \mathbf{D} \cdot (\epsilon_{n+1} - \epsilon_n^p), \quad \epsilon_{n+1} = \epsilon_n + \nabla^s \Delta \mathbf{u}. \quad (12)$$

With Eqs. (10) and (11), the stress tensor, σ_{n+1} , can then be computed as:

$$\sigma_{n+1} = \mathbf{I}_c^{-1} \cdot \sigma^{tr}, \quad \mathbf{I}_c = \mathbf{I} + u \mathbf{D} \mathbf{P}, \quad u = \frac{\Delta\gamma}{\varphi_{n+1}}. \quad (13)$$

Inserting this relation into the yield condition, Eq. (4) renders the following algorithmic consistency condition as:

$$f_{n+1} = \varphi_{n+1} - \sigma_{p,n+1} = 0 \tag{14} \quad I_1 = \lambda_1^2 + \lambda_2^2 + \lambda_3^2 \tag{21}$$

$$\text{with } \varphi_{n+1} = \left[\boldsymbol{\sigma}^{trT} \cdot \mathbf{I}_c^{-T} \cdot \mathbf{P} \cdot \mathbf{2I}_c^{-1} \cdot \boldsymbol{\sigma}^{tr} \right]^{1/2}, \sigma_p = \sigma_Y + R \tag{15} \quad \bar{I}_2 = J^{-4/3} I_2 \tag{22}$$

This furnishes a non-linear scalar equation, which will be solved with the Newton method. If the Newton iteration is used to solve the yield equation, the derivative of the yield function is needed. At the k iteration, this is given by:

$$\frac{df_k}{d(\Delta\gamma)} = \frac{d\varphi_k}{d(\Delta\gamma)} - R' \tag{16}$$

with, see Wali et al. [29]:

$$\frac{d\varphi}{d(\Delta\gamma)} = \mathbf{n} \cdot \mathbf{I}_c^{-1} [-\varphi u' \mathbf{Dn}] \tag{17}$$

$$u' = \frac{\sigma_p - R' \Delta\gamma}{\sigma_p^2} \tag{18}$$

The solution of Eq. (14) may then be effectively accomplished by the simple local iteration procedure and the whole integration algorithm is given in Table 1.

Mooney–Rivlin model

The rubber behavior is assumed to be hyper-elastic according to Mooney–Rivlin form. Hyper-elasticity postulates the existence of strain energy function W , which is defined per unit reference volume. For the Mooney–Rivlin model, the strain energy function W takes the form:

$$W = C_1(\bar{I}_1 - 3) + C_2(\bar{I}_2 - 3) + \frac{1}{D_1}(J - 1)^2 \tag{19}$$

$$\bar{I}_1 = J^{-2/3} I_1 \tag{20}$$

Table 1 Integration algorithm

(I) Compute trial elastic stress
 $\boldsymbol{\sigma}^{tr} = \mathbf{D} \cdot (\boldsymbol{\epsilon}_{n+1} - \boldsymbol{\epsilon}_n^p)$

(II) Find $\Delta\gamma$ by local iteration
 (1) $f_k = \varphi_k - \sigma_{p,k}$ $\varphi_k = \left[\boldsymbol{\sigma}^{trT} \cdot \mathbf{I}_c^{-T} \cdot \mathbf{P} \cdot \mathbf{I}_c^{-1} \cdot \boldsymbol{\sigma}^{tr} \right]^{1/2}$
 $\mathbf{I}_c = \mathbf{I} + u \mathbf{D} \mathbf{P}, u = \frac{\Delta\gamma}{\varphi_k}$
 (2) $f'_k = \frac{d\varphi_k}{d(\Delta\gamma)} - \sigma'_{p,k}$
 (3) $\Delta\gamma_{k+1} = \Delta\gamma_k - \frac{f_k}{f'_k}$
 (4) if $|f_k| > Tol$ then $k = k + 1$ go to (i)

(III) Update variables
 $\boldsymbol{\sigma}_{n+1} = \mathbf{I}_c^{-1} \cdot \boldsymbol{\sigma}^{tr}$

$$I_1 = \lambda_1^2 \lambda_2^2 + \lambda_2^2 \lambda_3^2 + \lambda_3^2 \lambda_1^2, \tag{23}$$

where C_1 and C_2 are empirically determined material constants, and \bar{I}_1 and \bar{I}_2 are the first and the second deviatoric strain component invariants.

J represents volume change $J = \det(\mathbf{F}) = \lambda_1 \lambda_2 \lambda_3$, where \mathbf{F} is the deformation gradient, for an incompressible material, $J = 1$.

C_1 , C_2 , and D_1 are material constants. Describe deviatoric component and D_1 describes compressibility. Compressibility can be defined by specifying nonzero values for D_1 , by setting the Poisson’s ratio to a value less than 0.5 or by providing test data that characterize the compressibility. All the Mooney–Rivlin constant will be determined through experimental compression test and numerical simulation test using Abaqus. By fitting the curves of these simulations with the curves of the experimental data, Abaqus calculates the hyper-elastic constants.

Material characterization

This section presents the summarized results of the experimental characterization of the AA1050-H14 aluminum sheet and the elastic cushion manufactured from polyurethane with different hardness 50, 70, and 90 shore A and the Natural Rubber.

Results of the tensile test used to characterize the aluminum sheet and the experimental setup are presented in Fig. 1.

The mechanical properties and Hill 48 coefficients resulted from these tests are summarized in Table 2.

In the literature, the most commonly used isotropic hardening laws are power type laws such as the Ludwig or Swift law or exponential laws. For our case, the law that best suited our material is the exponential law defined by the equation below. The different parameters are calculated by fitting the numerical curve with experimental result corresponding to specimen cut through the roller direction of the sheet metal.

$$R = 90 + 23,5(1 - e^{-412 \cdot \epsilon^p}) \tag{24}$$

To identify the hyper-elastic properties of the four elastomers used, compression tests are performed. The experimental setup and results are presented in Figs. 2 and 3.

After fitting the curves of ABAQUS simulations with curves of the experimental data, ABAQUS calculates the hyper-elastic constants. Results are summarized in Table 3.

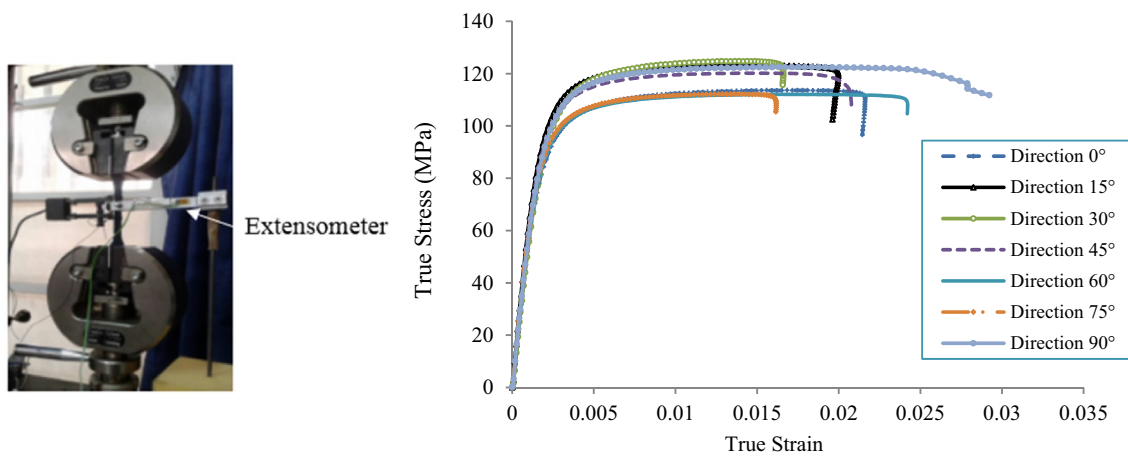


Fig. 1 a Uniaxial tensile test setup. b Hardening curves for AA 1050 at seven orientations

Table 2 AA1050 mechanical properties and anisotropy coefficients

Mechanical properties			Hill 48_R coefficients					
E (GPa)	$R_{p0.2}$ (MPa)	R_m (MPa)	G	H	F	N	L	M
57.42	114.88	117.71	0.69	0.31	0.64	1.52	1.52	1.52



Fig. 2 Compression test of the elastomer

Table 3 Mooney–Rivlin constants

Elastomer	Hardness Shore A	Mooney–Rivlin constantes	
		$C1$ (MPa)	$C2$ (MPa)
Polyurethane	50	0.302	0.067
	70	0.736	0.184
	90	2.824	0.706
Natural Rubber	70	2.307	0.157

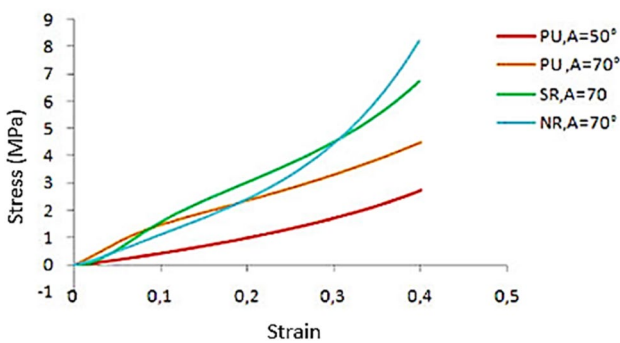


Fig. 3 Compression test results

The various parameters summarized in Tables 2 and 3 constitute data: first for the elastoplastic constitutive model with quadratic yield criterion of Hill 48 and isotropic hardening describing the material behavior model considered for the AA 1050-H14 aluminum sheet; second, for the

hyper-elastic behavior model considered for the rubber-pad cushion.

Experimental investigation

The experimental study presented throughout this section has two essential parts. The first presents the main results of the bending tests made using either the rigid die or the elastomer cushion with flexible materials of different hardness or grade. In the second part, a comparison between numerical and experimental results has been performed at the aim to validate the numerical model used along the last section.

Experimental setup

Three essential tools are used to compare bending using an elastic cushion with the classic bending procedure. A prismatic die (38 × 80 mm) having a U-shape groove in the middle (18 × 15 mm) where the elastomer cushion, with the same size as the U, will be embedded (Fig. 4c). This die

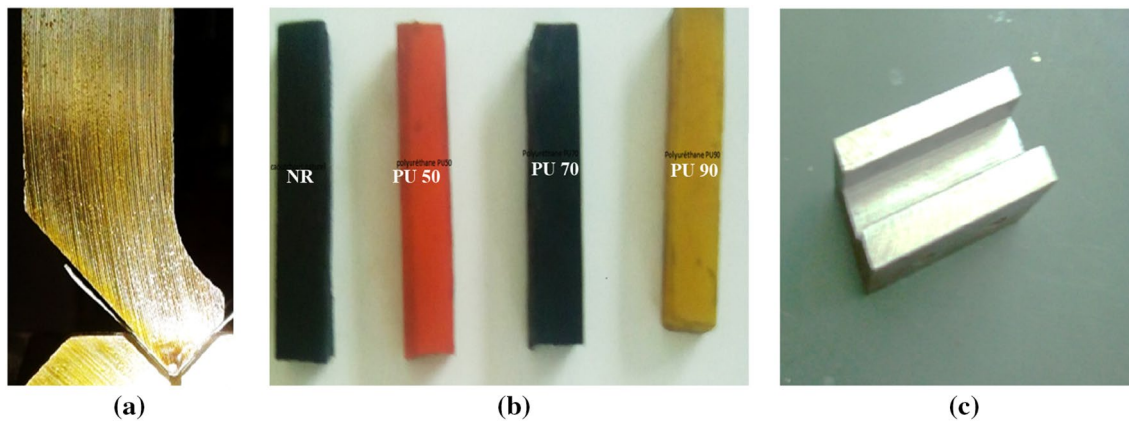


Fig. 4 Flexible bending process tooling: **a** punch, **b** elastomer, and **c** die

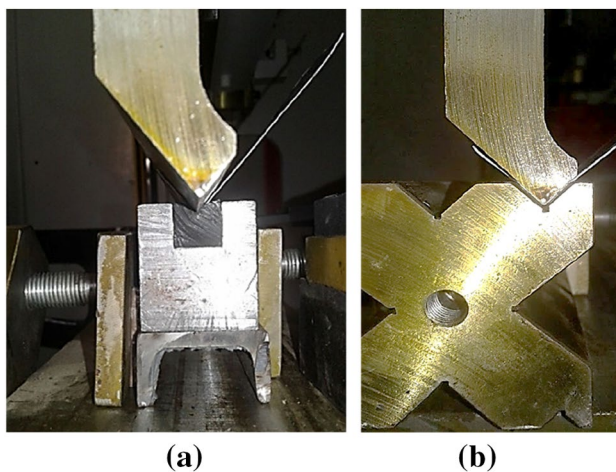


Fig. 5 Bending operation: **a** with elastic cushion and **b** conventional procedure

will replace the metallic V-die (Fig. 5b) on the hydraulic press machine. A punch tool with an angle of 86° and a radius 1 mm is used. Four types of elastomer (polyurethane 50, polyurethane 70, polyurethane 90, and Natural Rubber) (Fig. 4b) prepared by cutting to the dimensions of the U groove.

The bending operation presented was performed on the initial blank sheets 0.6 mm thick and having a dimensions $40 \text{ mm} \times 100 \text{ mm}$ cut through the rolling direction of the AA1050 aluminum sheet.

Results and discussion

Figure 6 depicts the classic bending procedure results. A poor surface condition was denoted, actually trace of the punch tool are marked over the contact surface. In fact, a

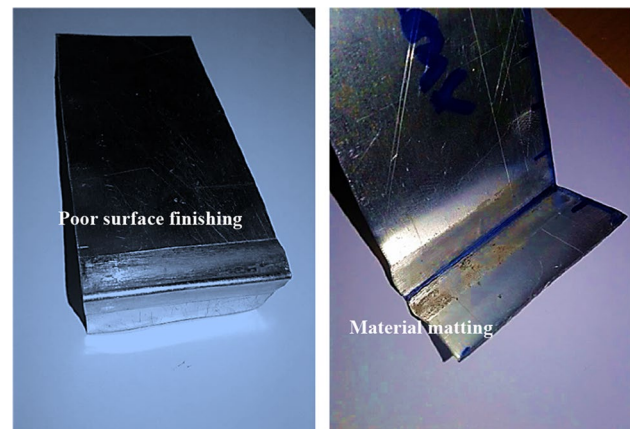


Fig. 6 Classic bending result

material matting caused by the rigid contact is denoted in this figure; during the application of the bending effort, the rigid tools crash the material through all the contact surfaces, especially in the case of thin sheets. This problem disappears when the elastomer cushion is used (Fig. 7). In fact using PU50, 70, 90, or the Natural Rubber as an elastic die, ameliorates the finishing quality of the manufactured part and avoids material matting and deformation certainly when the sheet is very thin or made from weak materials.

To verify the accuracy of the manufactured part, bent angles were measured using a protractor. Table 4 summarizes the different bent angles and springback values. The springback is calculated using the target angle 86° as reference, which is the punch angle. Analyzing the table, it can be denoted that with the PU70 and Natural Rubber NR, bent angle obtained is equal to the punch angle (angle 86° , which is the targeted angle). For PU50 and classic case, the angles were opened at, respectively, 87.5° and 88° . Whereas for the PU90, the bent was more opened (angle 101°); certainly

Fig. 7 Bending using the elastic cushion results



Table 4 Measured angles

Die	Measured angles	
	Bent angle (°)	Springback (°)
PU50	87.5	1.5
PU70	86	0
PU90	101	15
Natural Rubber	86	0
Rigid Die	88	2

here was the cause of an insufficient press effort to deform the elastomer sufficiently to our bending angle. Therefore, with this insufficient effort, the plastic deformation will not be sufficient to avoid a rapid springback. Note that during the experiments, we kept the same effort adjustment and the same Y punch displacement for all tests. In fact, for a given press effort, the springback phenomenon became more readable by increasing the elastomer hardness. If the hardness exceeds a certain limit, a new adjustment in the press machine is needed at the aim to increase the press effort.

Eventually, considering the springback phenomenon, elastic cushion made of PU70 or NR is more suited to bend with accuracy a thin aluminum sheet.

Validation against experimental results

At the aim to validate, the numerical model is used to simulate bending with elastic cushion, and results presented in the present section make a comparison between numerical and experimental results in term of thinning for the case of use of natural rubber NR and forming effort for the case of bending with an elastic cushion made from PU70.

According to Figs. 8 and 9, the numerical model used to simulate bending with elastomeric cushion is suitable to be used in this case of manufacturing operation. In fact, thinning and forming effort values generated from ABAQUS simulation are approximately in the same range of the experimental results, which confirm the efficiency of the numerical model to predict thinning or forming forces. However, small difference can be remarked, especially for

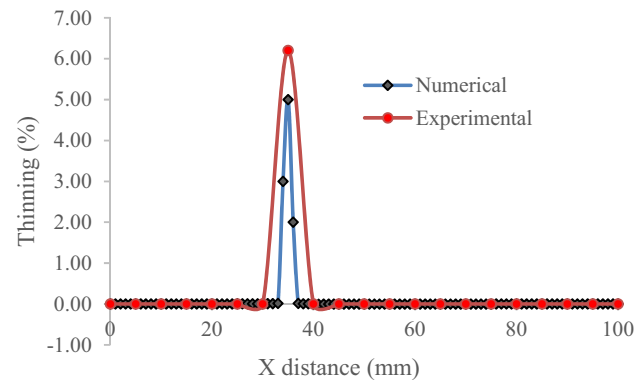


Fig. 8 Thinning variation along the roller direction for NR

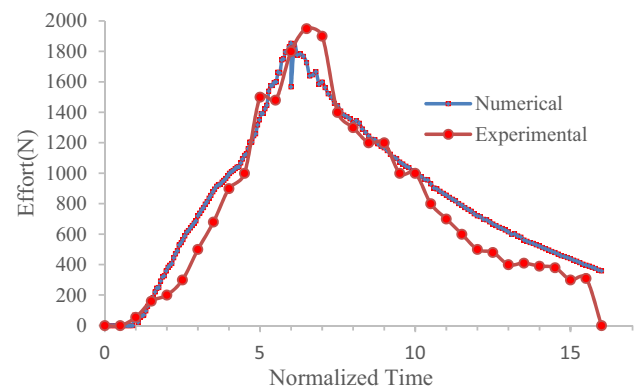


Fig. 9 Forming effort evolution for PU70

thinning parameter, which first can be explained by the experimental measurement errors. Analyzing the Fig. 8, the maximum of thinning is concentrated in a small zone, which is the zone of contact of the tool head (radius of 1 mm). In fact, because of the small dimension of this zone of contact, it is very difficult to make several measurements with the protractor for the experimental results. Second, the material behavior model used for simulations can be improved by integrating the material damage parameters and defining a frictional behavior that describes the real contact between rubber and sheet metal, which

demands advanced characterization tests to determine damage and friction models.

Numerical investigation

A 3-D finite-element code ABAQUS/Explicit (Fig. 10) was adopted to conduct a numerical comparison between classic bending and bending with elastic cushion made of different types of elastomeric materials. The blank, die, elastic cushion, and forming punch are modeled with shell elements (the die and punch are considered as rigid bodies). S4R shell elements are considered for the blank and the elastic cushion.

The various parameters presented in Sect. 3 constitute data for the behaviors of the material. For the aluminum sheet metal, elastoplastic model with Hill48 criteria and isotropic hardening is used. A Mooney–Rivlin model to describe the hyper-elastic behavior of the elastomeric cushions. Results concerning the forming effort, thinning, stress distribution, and springback are analyzed for the main goal to compare the classic procedure used to bend sheet metal and the use of elastic cushion.

The values of the force resulting from the contact pressure between the elements (sheet, punch, and die) during the bending operation are recorded in Fig. 11. We can denote from this figure that the use of an elastomer of high hardness increases considerably the amount of effort required to deform the flexible die and bend the sheet and at the desired angle and radius. At the certain limit, in the real case, the set effort (which is the press machine effort, chosen for the classic bending procedure) became insufficient to deform the elastomer, which corresponds to the case of PU90. In this case, plastic deformation is not sufficient to bend the blank sheet at the target angle

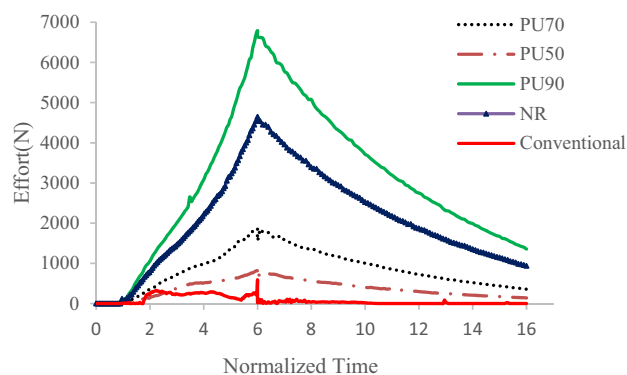


Fig. 11 Forming effort evolution for different case of Die

and the phenomenon of springback became more effective. Springback evolution plotted in Fig. 12 shows that conclusion. Whereas the best choice to avoid springback is the use of elastic die made of PU70.

The use of elastic cushion concentrates stresses in the center of bending radius (the main contact zone of the punch tool), as shown in Fig. 13. Contrariwise, to the classic bending procedure (Fig. 14), Von Mises stress is distributed over a large zone, the same zone where a poor surface quality is remarked in the experimental results. Evolution of thinning plotted in Fig. 15 shows the same conclusion; in fact, in conventional bending, thinning occurs in a large zone compared to elastic cushions results. In fact, in this case, the V-shaped walls of the rigid die crush the material, which leads to a large thinning zone. In the real case, it is the same zone where the material matting is denoted (Fig. 6). To reduce thinning during the bending operation using elastic cushion, low hardness elastic material should be chosen.

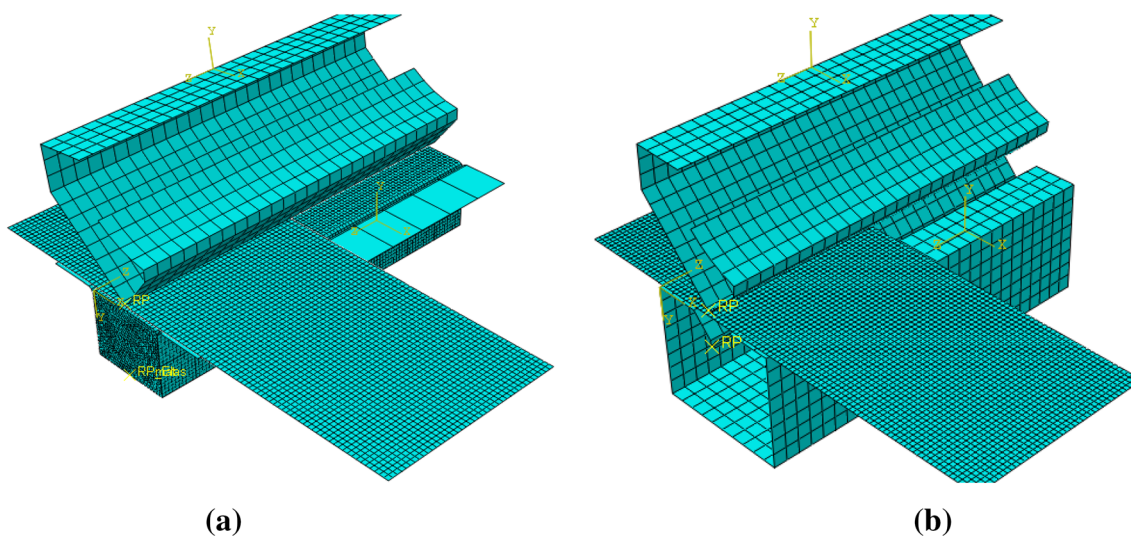


Fig. 10 Finite-element models: **a** with elastic cushion and **b** classic bending

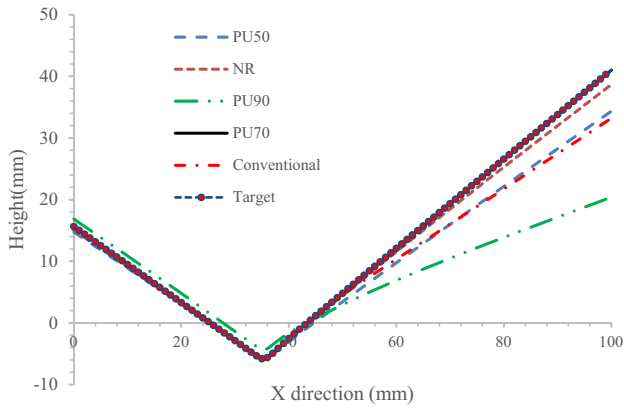


Fig. 12 Deformed shape after springback

Conclusion

In this study, the results of rubber-pad bending were investigated through experimental and FE analysis. These results were compared with the classic bending procedure using a rigid punch tool and V-die. In FE simulations, an elastoplastic constitutive model with quadratic yield criterion of Hill 48 and isotropic hardening behavior has been used. To model the rubber material behavior, a Mooney–Rivlin theory is used in the finite-element simulation. Based on experimental results, rubber-pad bending is an efficient solution to avoid material matting and poor surface quality encountered during the conventional bending operation. Polyurethane 70 shore A is the best elastic cushion in terms of surface quality and bent angle

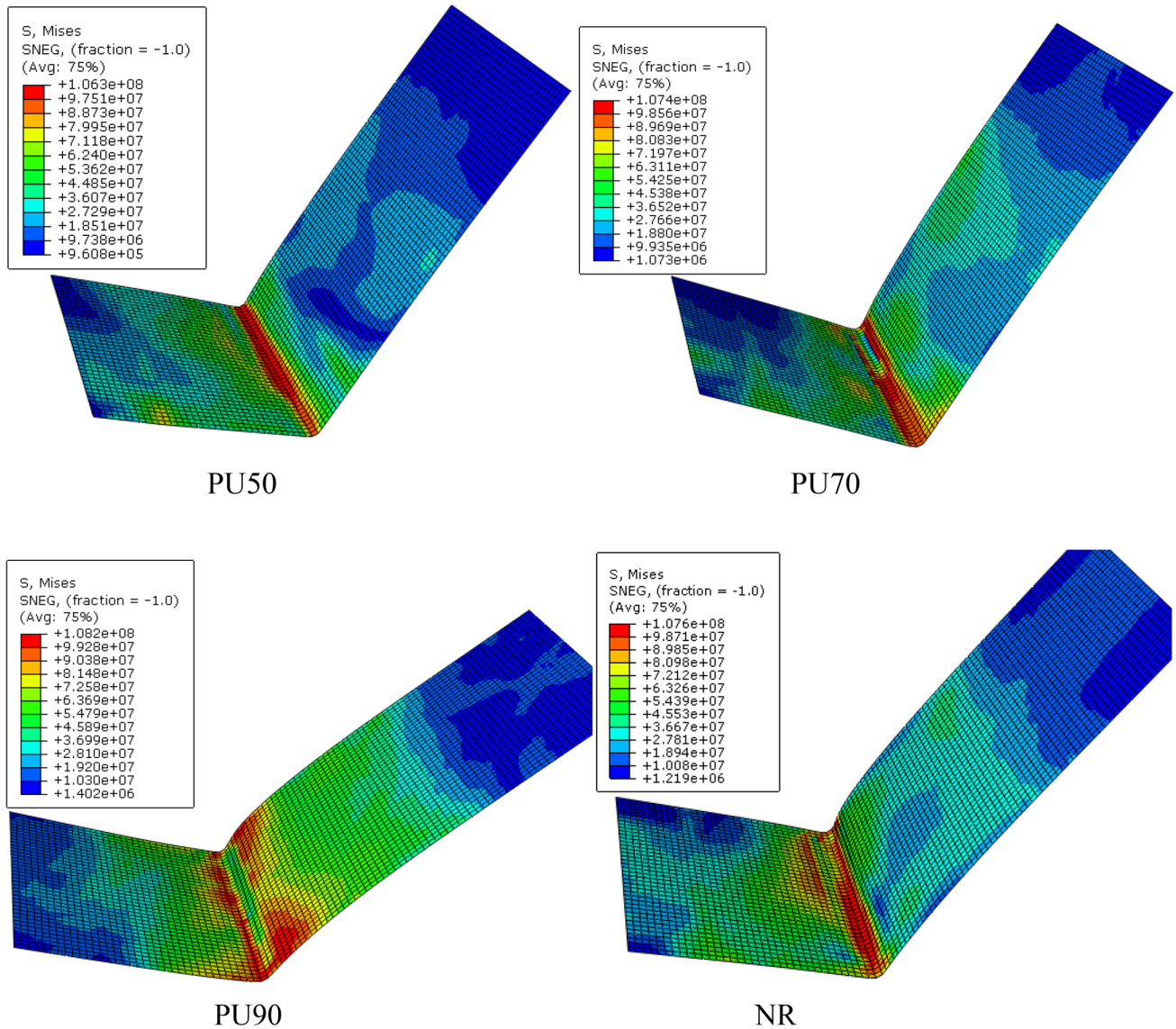


Fig. 13 Distribution of Von Mises stress for elastomeric die case

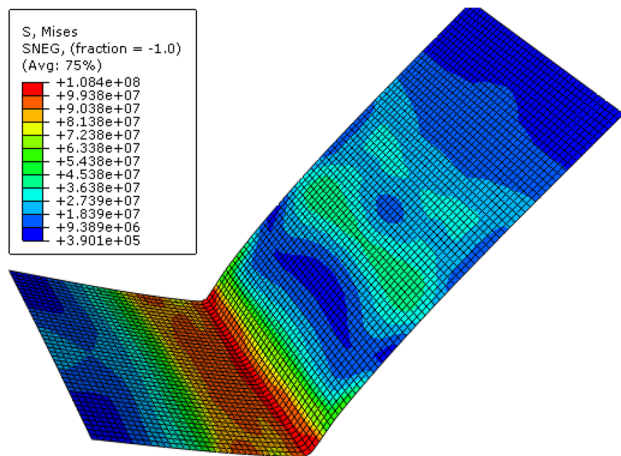


Fig. 14 Distribution of Von Mises stress for Rigid die case

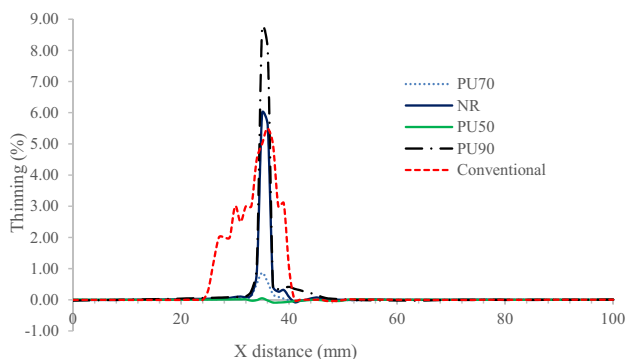


Fig. 15 Thinning evolution for the different case of die

accuracy. The use of this type of soft elastomeric cushion avoids springback, which is an important and decisive parameter in obtaining the desired geometry of the part and design of the corresponding tooling. From numerical results, it is clear that FE simulation is an important tool to get the better choice when elastomeric tooling is used in sheet metal-forming process. In fact, analyzing the main problem in bending processes, which is springback phenomenon, it is clear that elastic cushion made of PU70 has improved the bend part accuracy. Whereas if the elastomer hardness exceeds a certain limit, the conventional bending effort will not be sufficient to avoid a rapid springback encountered in our case when PU90 cushion is used. Well, in this case, the solution is to set a higher new effort value with the aim to obtain the target bend part.

Acknowledgements The authors extend their appreciation to the Deanship of Scientific Research at King Khalid University for funding this work through research groups program under grant number (R.G.P.1/68/40).

Compliance with ethical standards

Conflict of interest The authors have no conflict of interest.

References

- Giuseppe S (2001) A numerical and experimental approach to optimize sheet-stamping technologies: part II-Aluminum alloys rubber forming. *J Mater Des* 22:299–315
- Alberti N, Forcelllese A, Fratini L, Gabrielli F (1998) Sheet metal forming of titanium blanks using flexible media. *CIRP Ann Manuf Technol* 47:217–220
- Dirikolu MH, Akdemir E (2004) Computer aided modelling of flexible forming process. *J Mater Process Technol* 148:376–381
- Peng L, Hu P, Lai X, Mei DQ, Ni J (2009) Investigation of micro/meso sheet soft punch stamping process-simulation and experiments. *J Mater Des* 30:783–790
- Quadrini F, Santo L, Squeo EA (2010) Flexible forming of thin aluminum alloy sheets. *Int J Mod Manuf Technol* 2:79–84
- Liu Y, Hua L (2010) Fabrication of metallic bipolar plate for proton exchange membrane fuel cell by rubber pad forming. *J Power Sources* 195:3529–3535
- Sun Y, Wan M, Wu X (2013) Wrinkling prediction in rubber forming of Ti-15-3 alloy. *Trans Nonferrous Met Soc China* 23:3002–3010
- Belhassen L, Koubaa S, Wali M, Dammak F (2016) Numerical prediction of springback and ductile damage in rubber-pad forming process of aluminum sheet metal. *Int J Mech Sci* 117:218–226
- Ramezani M, Mohd Ripin Z, Ahmad R (2009) Computer aided modelling of friction in rubber-pad forming process. *J Mater Process Technol* 209:4925–4934
- Browne DJ, Battikha E (1995) Optimization of aluminum sheet forming using a flexible die. *J Mater Process Technol* 55:218–223
- Chen L, Chen H, Guo W, Chen G, Wang Q (2014) Experimental and simulation studies of springback in rubber forming using aluminum sheet straight flanging process. *Mater Des* 54:354–360
- Arnet H (1999) Advanced technology of plasticity. In: *Proceedings of the sixth ICTP* pp 2349
- Kwon HC, Im YT, Ji DC, Hrhee M (2001) The bending of an aluminum structural frame with a rubber pad. *J Mater Process Technol* 113:786–791
- Yoon SJ, Yang DY (2003) Development of a highly flexible incremental roll forming process for the manufacture of a doubly curved sheet metal. *CIRP Ann Manuf Technol* 52:201–204
- Shim DS, Yang DY, Han MS, Chung SW, Kim KH, Roh HJ (2008) Experimental study on manufacturing doubly curved plates using incremental rolling process. In: *Proceedings of the 9th International Conference on Technology of Plasticity*, Gyeongju pp 887–888.
- Li MZ, Hu ZQ, Cai ZY, Gong XP (2007) Method of efficient continuous plastic forming for freeform surface part. *J Jilin Univ* 37:489–494
- Lee JW, Kwon HC, Rhee MH, Im YT (2003) Determination of forming limit of a structural aluminum tube in rubber pad bending. *J Mater Process Technol* 140:487–493
- Liu Y, Hua L, Lan J, Wei X (2010) Studies of the deformation styles of the rubber-pad forming process used for manufacturing metallic bipolar plates. *J Power Sources* 195:8177–8184
- Chen L, Chen H, Guo W, Chen G, Wang Q (2013) Experimental and simulation studies of springback in rubber forming using aluminum sheet straight flanging process. *J Mater Des* 54:354–360

20. Liu H, Zhang G, Shen Z, Zhang W, Wang X (2017) Investigation of micro-bending of sheet metal laminates by laser-driven soft punch in warm conditions. *Micromachines* 8:224
21. Jin CK, Jeong MG, Kang CG (2014) Fabrication of titanium bipolar plates by rubber forming and performance of single cell using TiN-coated titanium bipolar plates. *Int J Hydrogen Energy* 39:21480–21488
22. Mars J, Ben Said L, Wali M, Dammak F (2018) Elasto-plastic modeling of low-velocity impact on functionally graded circular plates. *Int J Appl Mech* 10(4):1850038
23. Bouhamed A, Jrad H, Ben Said L, Wali M, Dammak F (2019) A non-associated anisotropic plasticity model with mixed isotropic–kinematic hardening for finite element simulation of incremental sheet metal forming process. *Int J Adv Manuf Technol* 100:929–940
24. Ben Said L, Mars J, Wali M, Dammak F (2016) Effects of the tool path strategies on incremental sheet metal forming process. *Mech Ind* 17:411
25. Ben Said L, Mars J, Wali M, Dammak F (2017) Numerical prediction of the ductile damage in single point incremental forming process. *Int J Mech Sci* 131–32:546–558
26. Koubaa S, Mars J, Wali M, Dammak F (2017) Numerical study of anisotropic behavior of Aluminum alloy subjected to dynamic perforation. *Int J Impact Eng* 101:105–114
27. Koubaa S, Belhassen L, Wali M, Fakhreddine Dammak F (2017) Numerical investigation of the forming capability of bulge process by using rubber as a forming medium. *Int J Adv Manuf Tech* 92:1839–1848
28. Autay R, Koubaa S, Wali M, Dammak F (2018) Numerical implementation of coupled anisotropic plasticity-ductile damage in sheet metal forming process. *J Mech* 34:417–430
29. Wali M, Chouchene H, Ben Said L, Dammak F (2015) One-equation integration algorithm of a generalized quadratic yield function with Chaboche non-linear isotropic/kinematic hardening. *Int J Mech Sci* 92:223–232
30. Mars J, Wali M, Jarraya A, Dammak F, Dhiab A (2015) Finite element implementation of an orthotropic plasticity model for sheet metal in low velocity impact simulations. *Thin Walled Struct* 89:93–100
31. Belhassen L, Koubaa S, Wali M, Dammak F (2017) Anisotropic effects in the compression beading of aluminum thin-walled tubes with rubber. *Thin-Walled Struct*. <https://doi.org/10.1016/j.tws.2017.08.010>
32. Wali M, Autay R, Mars J, Dammak F (2016) A simple integration algorithm for a non-associated anisotropic plasticity model for sheet metal forming. *Int J Numer Methods Eng* 107:183–204
33. Ben SL, Belhassen L, Mars J, Wali M (2018) On the use of NC milling and turning machines in spif process of asymmetric parts: numerical investigation. Design and modeling of mechanical systems—III: CMSM 2017: lecture notes in mechanical engineering. Springer, Cham
34. Ben SL, Wali M, Dammak F (2015) Numerical simulation of incremental sheet metal forming process. Multiphysics modeling and simulation for systems design and monitoring. MMSSD 2014. Applied condition monitoring. Springer, Cham
35. Hill R (1948) A theory of the yielding and plastic flow of anisotropic metals. *Proc Roy Soc Lond A* 193:281–297

Publisher's Note Springer Nature remains neutral with regard to jurisdictional claims in published maps and institutional affiliations.